

Long non-coding RNA MEG3 knockdown alleviates hypoxia-induced injury in rat cardiomyocytes via the miR-325-3p/TRPV4 axis

YA ZHOU^{1*}, XIANGUO LI^{2*}, DONG ZHAO³, XINYA LI⁴ and JIANJUN DAI¹

Departments of ¹Cardiology, ²Ultrasound and ³Medical Imaging, Jinxiang People's Hospital, Jining, Shandong 272200; ⁴Department of Endocrinology, Jining No.1 People's Hospital, Jining, Shandong 272000, P.R. China

Received November 15, 2019; Accepted October 13, 2020

DOI: 10.3892/mmr.2020.11656

Abstract. Acute myocardial infarction (AMI) is a common cardiac disease. Long non-coding RNA maternally expressed 3 (MEG3) is associated with cellular processes in numerous complicated diseases, including AMI. However, the mechanism underlying MEG3 in myocardial hypoxia is not completely understood. The present study aimed to investigate the underlying mechanism of MEG3 in myocardial hypoxia. The expression levels of hypoxia-inducible factor 1 α (HIF1 α), MEG3, microRNA (miR)-325-3p, and transient receptor potential cation channel subfamily V member 4 (TRPV4) in hypoxia-treated H9c2 cells were detected via reverse transcription-quantitative PCR. The protein expression levels of HIF1 α , Bcl-2, Bax, cleaved caspase-3 and TRPV4 were detected via western blotting. Cell viability and apoptosis were assessed by performing an MTT assay and flow cytometry, respectively. Lactate dehydrogenase (LDH) release was monitored by conducting an LDH determination assay. The Dual-Luciferase reporter assay was performed to verify the targeted relationship between miR-325-3p and MEG3 or TRPV4. The expression levels of MEG3 and TRPV4 were significantly increased, whereas miR-325-3p expression levels were significantly decreased in hypoxic H9c2 cells compared with normoxic H9c2 cells. In addition, miR-325-3p was downregulated by MEG3 compared with the vector group, and miR-325-3p targeted TRPV4 in hypoxia-treated H9c2 cells. The results indicated that MEG3 knockdown attenuated hypoxia-stimulated injury in H9c2 cells by regulating miR-325-3p. TRPV4

knockdown also mitigated hypoxia-induced injury in H9c2 cells via miR-325-3p. Furthermore, compared with the vector group, MEG3 increased TRPV4 expression in hypoxia-treated H9c2 cells by sponging miR-325-3p. Collectively, the results of the present study suggested that MEG3 modulated TRPV4 expression to aggravate hypoxia-induced injury in rat cardiomyocytes by sponging miR-325-3p.

Introduction

Acute myocardial infarction (AMI) is caused by acute and persistent ischemia, as well as hypoxia of the coronary artery (1). The mortality of AMI in China has increased to 1 million per year in the past two decades based on an analysis of hospital data from 1990 to 2010 (2). Therefore, it is necessary to explore the regulatory mechanism underlying AMI development for the improvement of therapeutic strategies.

Long non-coding RNAs (lncRNAs) are a form of long RNAs (>200 nucleotides) with no translation ability but an ability to affect gene expression at the transcriptional level (3). A number of studies have demonstrated that lncRNAs are associated with the development of AMI. For example, lncRNA metastasis associated lung adenocarcinoma transcript 1 facilitated AMI development via the miR-320/phosphatase and tensin homolog axis (4). In addition, another study revealed that hypoxia stimulated the expression of Testis-Specific Transcript, Y-Linked 15 (TTY-15), and TTY-15 knockdown refrained hypoxia-induced injury (5). Moreover, it has been reported that maternally expressed 3 (MEG3) is associated with AMI development (6,7); however, the regulatory mechanism underlying MEG3 in AMI is not completely understood.

MicroRNAs (miRNAs/miRs), a type of small RNAs (~22 nucleotides) without translation capacity, negatively regulate target genes expression by mediating mRNA degradation or repressing mRNA translation (8). A number of miRNAs have been identified to be involved in AMI development. For example, Chen *et al* (9) demonstrated that miR-133 improved cardiac injury in AMI. In addition, another study indicated that miR-145 downregulation in plasma was related to AMI (10) and miR-325-3p was also reported to participate in the development of AMI (11).

Correspondence to: Dr Ya Zhou, Department of Cardiology, Jinxiang People's Hospital, 117 Jinfeng East Road, Jining, Shandong 272200, P.R. China
E-mail: zy15563198696@163.com

*Contributed equally

Key words: maternally expressed 3, microRNA-325-3p, transient receptor potential cation channel subfamily V member 4, cardiomyocytes, hypoxia

Transient receptor potential cation channel subfamily V member 4 (TRPV4) is a gene locus on human chromosome 12q24.11, which encodes a nonselective cation channel protein that is important for systemic osmotic pressure (12). Dysregulation of TRPV4 has been reported in AMI (13). However, the regulatory mechanism underlying miR-325-3p and TRPV4 in AMI has not been previously reported. Therefore, the present study investigated the functions and mechanisms underlying MEG3 in hypoxia-induced injury.

Materials and methods

Cell culture and treatment. The rat cardiomyocyte cell line (H9c2) was purchased from Procell Life Science & Technology Co., Ltd. and cultured in DMEM (Beijing Solarbio Science & Technology Co., Ltd.) supplemented with 10% FBS (Genetimes Technology, Inc.) in an incubator at 37°C. H9c2 cells were divided into two groups: i) Normoxia group (cultured with 95% air and 5% CO₂); and ii) hypoxia group (cultured with 94.5% N₂, 5% CO₂ and 0.5% O₂).

Reverse transcription-quantitative PCR (RT-qPCR). Total RNA from H9c2 cells was extracted using TriQuick Reagent (Beijing Solarbio Science & Technology Co., Ltd.). Reverse transcription for lncRNAs and mRNAs was performed using AMV Reverse Transcriptase (Beijing Solarbio Science & Technology Co., Ltd.), whereas reverse transcription for miRNA was performed using the TaqMan miRNA kit (Applied Biosystems; Thermo Fisher Scientific, Inc.). Total RNA (1 µg), 1 µl Oligo (dT), 0.5 µl dNTPs, 2 µl 5 X reaction buffer, 1 µl AMV Reverse Transcriptase and 4.5 DEPC H₂O was mixed and followed by reverse transcription (42°C for 60 min). Subsequently, qPCR was performed using SYBR® Premix Ex Taq II (Takara Biotechnology Co., Ltd.). The following parameters were used for qPCR: 1 cycle at 98°C for 3 min, followed by 40 cycles for 15 sec at 94°C, for 30 sec at 60°C, and for 1 min at 72°C. The expression of mRNA and miRNA were quantified using the 2^{-ΔΔC_q} method (14) and normalized to the internal reference genes β-actin and U6, respectively. The following primers (synthesized by BGI Group) were used for qPCR: HIF1α forward, 5'-CTGACCCTGCACTCAATC AAG-3' and reverse, 5'-TGGGACTATTAGGCTCAGGTG-3'; MEG3 forward, 5'-GGCAGGATCTGGCATAGAGG-3' and reverse, 5'-CGAGTCAGGAAGCAGTGGGT-3'; miR-325-3p forward, 5'-GCCAGCACCTTCACAAAGTAGC and reverse, 5'-CCATGCTAGACAACAGCTCTG-3'; TRPV4 forward, 5'-CCCGAGAGAACACCAAGTTTG-3' and reverse, 5'-GAC CGTCATTGTAAAGCACAGTCT-3'; β-actin forward, 5'-CGT TGACATCCGTAAAGACC-3' and reverse, 5'-TAGAGCCAC CAATCCACACA-3'; and U6 forward, 5'-CTCGCTTCGGCA GCACA-3' and reverse, 5'-AACGCTTCACGAATTTGCGT-3'.

Western blotting. Total protein was extracted from H9c2 cells using a protein extraction kit (Beyotime Institute of Biotechnology). Total protein was quantified using a bicincho-nic protein assay kit (Beyotime Institute of Biotechnology). The protein samples (35 µg per lane) were separated via 10% SDS-PAGE and transferred onto PVDF membranes (EMD Millipore). The membranes were blocked in 5% skimmed milk for 4 h at 37°C, and incubated for 12 h at 4°C with the

following primary antibodies (all purchased from Abcam): HIF1α (cat. no. ab51608, 1:400), Bcl-2 (cat. no. ab196495, 1:1,000), Bax (cat. no. ab104156, 1:1,000), cleaved caspase-3 (cat. no. ab2302, 1:1,000), TRPV4 (cat. no. ab39260, 1:1,000) and β-actin (cat. no. ab8227, 1:1,000). Subsequently, the membranes were incubated with a secondary antibody goat anti-rabbit IgG H&L (HRP) (cat. no. ab205718, 1:20,000; Abcam) for 2 h at 37°C. Protein bands were visualized using an ECL kit (Beyotime Institute of Biotechnology). β-actin was used as the loading control. Quantification of band intensities by densitometry was performed using the ImageJ software version (V1.8.0._172; National Institutes of Health).

Cell transfection. The small interfering siRNA targeted against MEG3 (si-MEG3; 5'-GCTTCTCGAGGCCTGTCT ATT-3'), siRNA targeted against TRPV4 (si-TRPV4; 5'-CGU GUCCUUCUACAUAATT-3'), negative control (NC) siRNA (si-NC), miR-325-3p mimic (miR-325-3p), mimic NC (miR-NC), miR-325-3p inhibitor (anti-miR-325-3p) and inhibitor NC (anti-miR-NC) were purchased from Shanghai GeneChem Co., Ltd. The fragment of MEG3 was inserted into the pcDNA vector to construct the MEG3 overexpres-sion plasmid (MEG3). The blank load pcDNA vector was used as the negative control. Cells (4x10⁵ cells/well) were transfected with siRNA (10 nM at final concentration), mimic (25 nM at final concentration), inhibitor (50 nM at final concentration), overexpression plasmid (4 µg) or equal amounts of NCs using Lipofectamine® 2000 (Invitrogen; Thermo Fisher Scientific, Inc.). Cells were replaced with fresh medium 6 h after transfection before the hypoxia group received hypoxia treatment for 24 h after transfection for subsequent experiments.

MTT assay. An MTT assay (Beijing Solarbio Science & Technology Co., Ltd.) was performed to detect H9c2 cell viability. H9c2 cells were seeded (5x10³ cells/well) into a 96-well plate and incubated at 37°C for 24 h. Then, 24 h after transfection, cells were incubated for 0, 24, 48 or 72 h in hypoxic conditions. Subsequently, cells were incubated with MTT for 4 h at 37°C. DMSO was added to dissolve the formazan. The absorbance of each well was measured at a wavelength of 490 nm using a microplate reader.

Flow cytometry analysis of cell apoptosis. The Annexin V/prop-idium iodide cell apoptosis analysis kit (Wuhan Servicebio Technology Co., Ltd.) was utilized to assess H9c2 cell apop-tosis (early + late apoptosis). Briefly, H9c2 cells (1x10⁶) were incubated in hypoxic conditions for 24 h and then resuspended in binding buffer. Subsequently, cells were incubated with Annexin V for 10 min at 37°C in darkness and then stained with PI for 5 min at 37°C in the dark. H9c2 cell apoptosis was assessed using an ACEA NovoCyt flow cytometer (2060R, ACEA; Agilent Technologies, Inc.) with ACEA NovoExpress software version 1.2.1 (ACEA; Agilent Technologies, Inc.).

Lactate dehydrogenase (LDH) determination assay. The LDH Activity Detection kit (cat. no. BC0685; Beijing Solarbio Science & Technology Co., Ltd.) was used to detect LDH release in H9c2 cells according to the manufacturer's instructions.

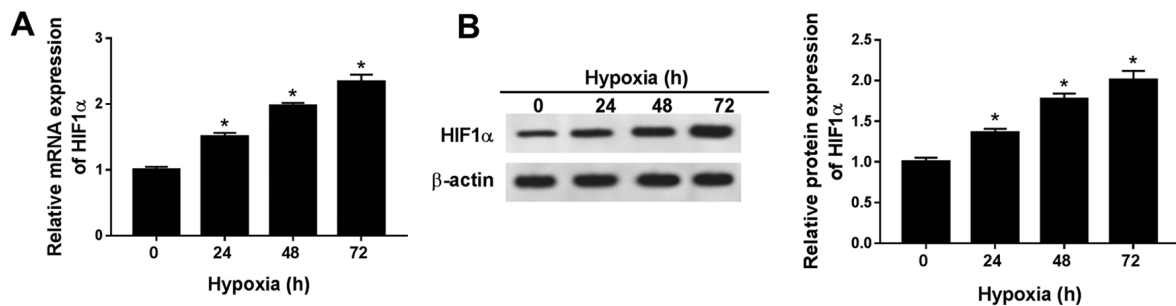


Figure 1. HIF1 α expression levels are significantly increased in hypoxia-treated H9c2 cells. HIF1 α (A) mRNA and (B) protein expression levels in H9c2 cells after hypoxia treatment for 24, 48 or 72 h. $n=3$. * $P<0.05$. HIF, hypoxia-inducible factor.

Dual-Luciferase reporter assay. The interaction between miR-325-3p and MEG3 or TRPV4 was predicted using LncBase Predicted (version 2; carolina.imis.athena-innovation.gr/diana_tools/web/index.php?r=lncbasev2%2Findex-predicted) or Targets can Human 7.1 (www.targetscan.org) online databases, respectively. The wild-type (WT) and mutant (MUT) sequences of MEG3 or the 3'-untranslated regions (3'-UTRs) of TRPV4 were inserted into the pmirGLO vector (Hunan YouBio Medical Device Co., Ltd.) to construct WT-MEG3, MUT-MEG3, WT-TRPV4-3'UTR and MUT-TRPV4-3'UTR luciferase reports, respectively. H9c2 cells (4×10^5 cells/well) were co-transfected with WT-MEG3 (2 μ g), MUT-MEG3 (2 μ g), WT-TRPV4-3'UTR (2 μ g) or MUT-TRPV4-3'UTR (2 μ g) and miR-325-3p (25 nM at final concentration) or miR-NC (25 nM at final concentration) using Lipofectamine[®] 2000 (Invitrogen; Thermo Fisher Scientific, Inc.). Cells were replaced with fresh medium 6 h after transfection before the hypoxia group received hypoxia treatment 24 h after transfection for subsequent experiments. Luciferase activities were detected 48 h after transfection using the Dual-Lucy Assay kit (Beijing Solarbio Science & Technology Co., Ltd.). *Renilla* luciferase activities were normalized as control.

Statistical analysis. Quantitative data from three independent repeats are presented as the mean \pm SD. Comparisons between two groups or among multiple groups were analyzed using the unpaired Student's t-test or one-way ANOVA followed by Tukey's post hoc test, respectively. Statistical analyses were performed using GraphPad Prism software (version 7; GraphPad Software, Inc.). $P<0.05$ was considered to indicate a statistically significant difference.

Results

HIF1 α expression levels are significantly increased in hypoxic H9c2 cells. To establish a hypoxic rat cell model, H9c2 cells were cultured in 0.5% O₂ conditions. HIF1 α is an indicator of hypoxia (15), thus the expression levels of HIF1 α were detected in H9c2 cells after hypoxia treatment for 0, 24, 48 or 72 h. The mRNA and protein expression levels of HIF1 α were significantly increased in H9c2 cells after hypoxia treatment for 24, 48 and 72 h compared with normoxic H9c2 cells (hypoxia treatment for 0 h; Fig. 1A and B). The results indicated that the hypoxia-induced cardiomyocyte model was successfully established. As hypoxia treatment over a long duration may result in irreversible damage to H9c2

cells, hypoxia treatment for 24 h was selected for subsequent experiments.

MEG3 knockdown mitigates hypoxia-induced injury in H9c2 cells. The present study demonstrated that lncRNA MEG3 expression was significantly increased in a time-dependent manner under hypoxic conditions compared with normoxic H9c2 cells (Fig. 2A). In addition, the expression levels of MEG3 were significantly lower in hypoxia-treated H9c2 cells transfected with si-MEG3 compared with the si-NC group, indicating the transfection efficiency of si-MEG3 (Fig. 2B). Additionally, compared with normoxic H9c2 cells, cell viability was significantly reduced under hypoxic conditions, which was inhibited by transfection with si-MEG3 (Fig. 2C). Furthermore, hypoxia treatment significantly induced H9c2 cell apoptosis compared with normoxic H9c2 cells, and si-MEG3 attenuated hypoxia-induced apoptosis compared with si-NC (Fig. 2D). Also, compared with normoxic H9c2 cells, the protein expression levels of proapoptotic factors (Bax and cleaved caspase-3) were significantly increased under hypoxic conditions compared with normoxic conditions, but partly reversed by si-MEG compared with si-NC. By contrast, compared with normoxic H9c2 cells, the expression levels of the antiapoptotic marker Bcl-2 were significantly decreased in hypoxic H9c2 cells, resulting in a decreased Bcl2/Bax ratio and MEG3 knockdown partially reversed hypoxia-induced alterations to the Bcl2/Bax ratio compared with si-NC (Fig. 2E). LDH is related to cardiomyocytes injury (16), thus the release of LDH under hypoxic conditions was also monitored. Compared with normoxic H9c2 cells, LDH release was significantly increased in hypoxia-treated H9c2 cells, but significantly reduced in hypoxia-treated H9c2 cells transfected with si-MEG3 compared with H9c2 cells transfected with si-NC (Fig. 2F). The results suggested that MEG3 knockdown alleviated hypoxia-induced injury in H9c2 cells.

miR-325-3p negatively interacts with MEG3 in hypoxic H9c2 cells. To elucidate the mechanism underlying MEG3 in hypoxic cardiomyocytes, LncBase Predicted was used to identify the putative target of MEG3. Based on the bioinformatics analysis, miR-325-3p was identified as a potential target of lncRNA MEG3, and the difference in expression of miR-325-3p was the most significant among the candidate miRNAs in si-MEG treated cells (data not shown). As shown in Fig. 3A, miR-325-3p displayed complementary sequences with MEG3. The Dual-Luciferase reporter assay results

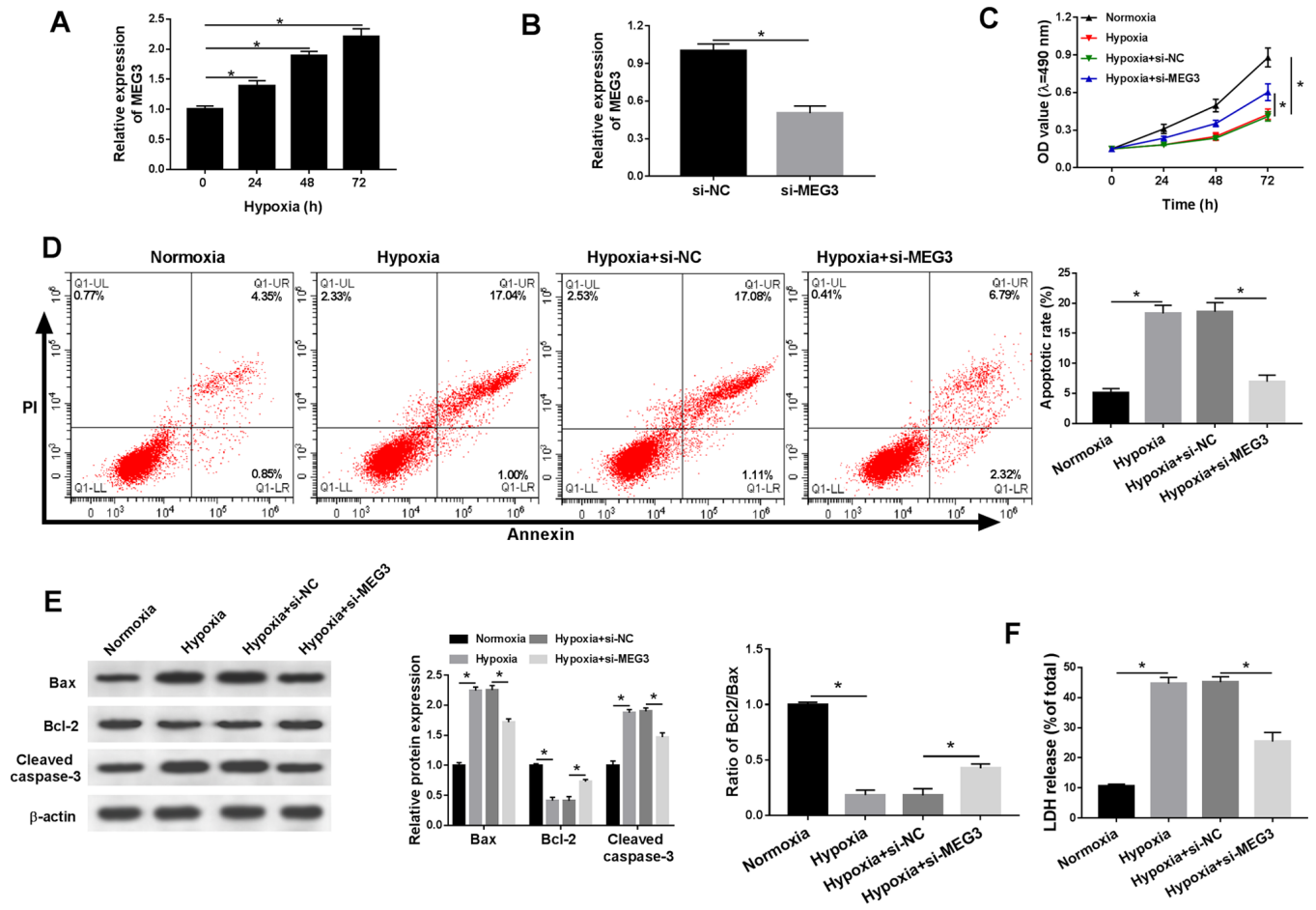


Figure 2. MEG3 knockdown alleviates hypoxia-induced injury in H9c2 cells. (A) MEG3 mRNA expression levels in H9c2 cells after hypoxia treatment for 0, 24, 48 or 72 h. (B) MEG3 mRNA expression levels in hypoxia-treated H9c2 cells transfected with si-NC or si-MEG3. H9c2 cells were cultured in normoxic or hypoxic conditions and then transfected with si-NC or si-MEG3. (C) Cell viability was assessed by performing an MTT assay. (D) Cell apoptosis was assessed via flow cytometry. (E) Protein expression levels of Bax, Bcl-2 and cleaved caspase-3 were detected via western blotting. (F) LDH release was measured via performing the LDH determination assay. $n=3$. * $P<0.05$. MEG3, maternally expressed 3; si, small interfering RNA; NC, negative control; OD, optical density; LDH, lactate dehydrogenase.

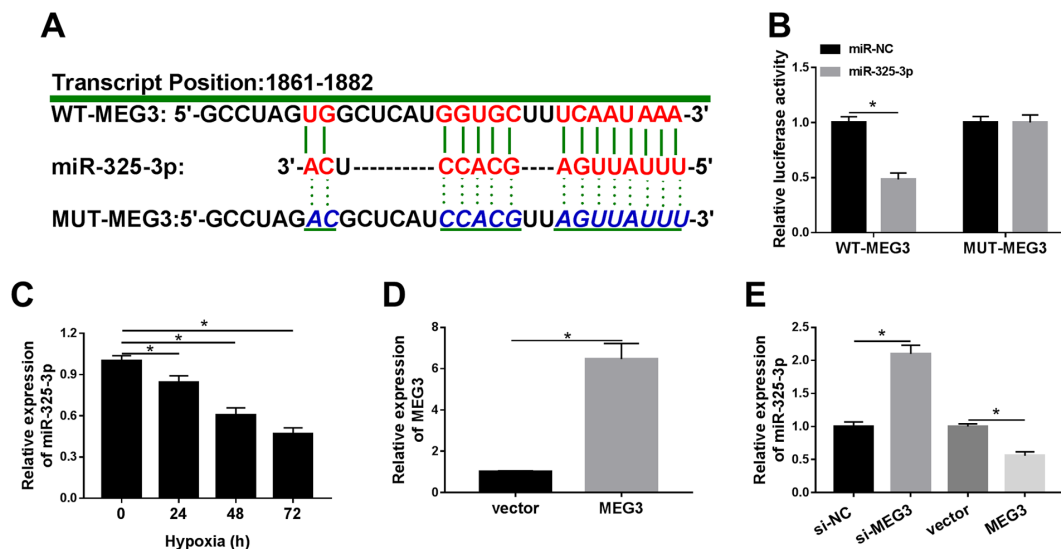


Figure 3. miR-325-3p negatively interacts with MEG3 in hypoxia-treated H9c2 cells. (A) The complementary binding sites between MEG3 and miR-325-3p, as well as the mutant sequences of MEG3. (B) The luciferase activities of WT-MEG3 and MUT-MEG3 in hypoxia-treated H9c2 cells transfected with miR-325-3p or miR-NC. (C) miR-325-3p expression levels in H9c2 cells after hypoxia treatment for 24, 48 or 72 h. (D) MEG3 expression levels in hypoxia-treated H9c2 cells transfected with vector or MEG3. (E) miR-325-3p expression levels in hypoxia-treated H9c2 cells transfected with si-NC, si-MEG3, vector or MEG3. $n=3$. * $P<0.05$. miR, microRNA; MEG3, maternally expressed 3; WT, wild-type; MUT, mutant; NC, negative control; si, small interfering RNA.

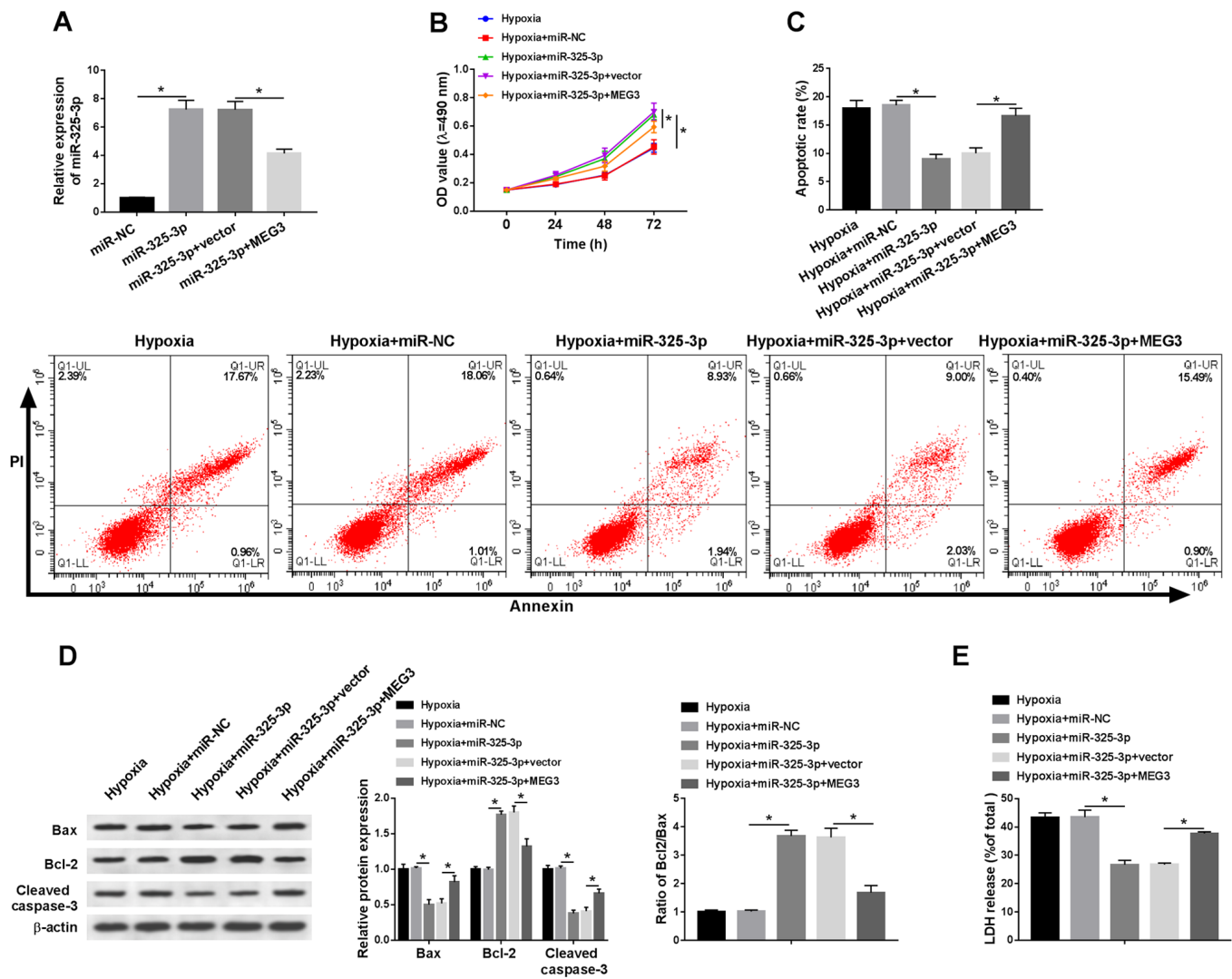


Figure 4. miR-325-3p overexpression reduces hypoxia-induced injury in H9c2 cells by downregulating MEG3. H9c2 cells were transfected with miR-NC, miR-325-3p, miR-325-3p + vector or miR-325-3p + MEG3, and then cultured in hypoxic conditions. (A) miR-325-3p expression levels following transfection. (B) Cell viability was evaluated by performing an MTT assay. (C) Cell apoptosis was assessed via flow cytometry. (D) Protein expression levels of Bax, Bcl-2 and cleaved caspase-3 were detected via western blotting. (E) LDH release was measured by performing the LDH determination assay. n=3. *P<0.05. miR, microRNA; MEG3, maternally expressed 3; NC, negative control; LDH, lactate dehydrogenase; OD, optical density.

demonstrated that miR-325-3p significantly decreased the luciferase activity of WT-MEG3 in hypoxia-treated H9c2 cells compared with the miR-NC group, whereas the luciferase activity of MUT-MEG3 was not significantly altered by transfection with miR-325-3p compared with miR-NC (Fig. 3B). In addition, the expression levels of miR-325-3p were significantly downregulated in hypoxia-treated H9c2 cells compared with normoxic H9c2 cells (Fig. 3C). Subsequently, MEG3 was overexpressed in hypoxia-induced H9c2 cells by transfection with MEG3. The RT-qPCR results confirmed the transfection efficiency of MEG3 (Fig. 3D). In addition, the expression levels of miR-325-3p were significantly increased in hypoxia-treated H9c2 cells transfected with si-MEG3 compared with hypoxia-treated H9c2 cells transfected with si-NC. By contrast, miR-325-3p expression levels were significantly decreased in the MEG3 group compared with the vector group in hypoxia-treated H9c2 cells (Fig. 3E). The results suggested that MEG3 reduced

the expression levels of miR-325-3p in hypoxia-treated H9c2 cells.

miR-325-3p overexpression improves hypoxia-induced injury in H9c2 cells by downregulating MEG3. To explore whether MEG3-associated hypoxia injury was mediated by miR-325-3p, rescue experiments were performed. The expression levels of miR-325-3p were detected in hypoxia-treated H9c2 cells. Compared with the miR-NC group, the expression levels of miR-325-3p were significantly elevated in miR-325-3p-transfected H9c2 cells under hypoxic conditions, which was partially inhibited by MEG3 compared with the vector group (Fig. 4A). In addition, MEG3 reduced miR-325-3p-mediated effects on cell viability in H9c2 cells under hypoxic conditions (Fig. 4B). Additionally, the rate of apoptosis and LDH release were significantly decreased in hypoxia-treated H9c2 cells transfected with miR-325-3p compared with the hypoxia + miR-NC group, which was

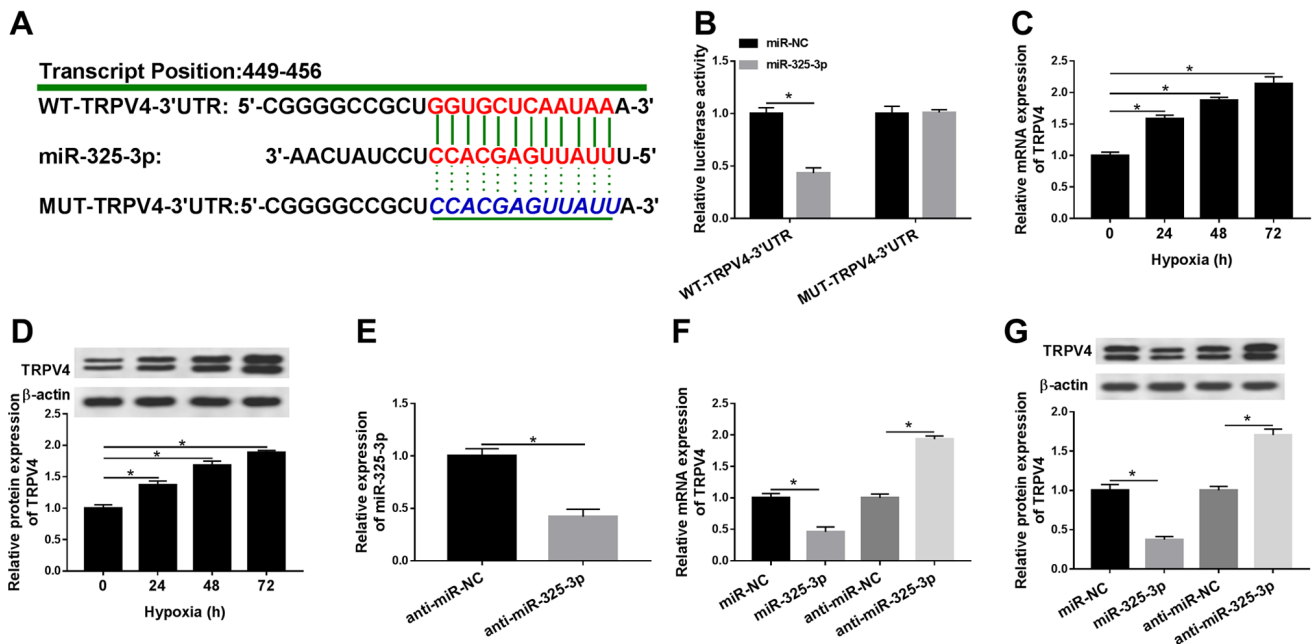


Figure 5. TRPV4 is a candidate target for miR-325-3p in hypoxia-treated H9c2 cells. (A) The complementary binding sites between TRPV4 and miR-325-3p, as well as the mutant sequences of TRPV4. (B) The luciferase activities of WT-TRPV4-3'UTR and MUT-TRPV4-3'UTR in hypoxia-treated H9c2 cells transfected with miR-325-3p or miR-NC. TRPV4 (C) mRNA and (D) protein expression levels in H9c2 cells after hypoxia treatment for 24, 48 or 72 h. (E) miR-325-3p expression levels in hypoxia-treated H9c2 cells transfected with anti-miR-NC or anti-miR-325-3p. TRPV4 (F) mRNA and (G) protein expression levels in hypoxia-treated H9c2 cells transfected with miR-NC, miR-325-3p, anti-miR-NC or anti-miR-325-3p. $n=3$. * $P<0.05$. TRPV4, transient receptor potential cation channel subfamily V member 4; miR, microRNA; WT, wild-type; UTR, untranslated region; MUT, mutant; NC, negative control.

partially recovered in hypoxia-treated H9c2 cells co-transfected with miR-325-3p and MEG3 compared with the hypoxia + miR-325-3p + vector group (Fig. 4C and E). In addition, MEG3 reversed miR-325-3p-mediated downregulation of Bax and cleaved caspase-3 protein expression levels, and attenuated miR-325-3p-mediated upregulation of Bcl-2 protein expression levels in hypoxia-treated H9c2 cells (Fig. 4D). The results suggested that MEG3 aggravated hypoxia-induced injury in H9c2 cells by regulating miR-325-3p.

TRPV4 is a candidate target of miR-325-3p in hypoxia-treated H9c2 cells. To further investigate the mechanism underlying miR-325-3p in hypoxia-treated cardiomyocytes, the potential candidate was identified using TargetScan. As shown in Fig. 5A, the 3'UTR of TRPV4 displayed a complementary base pairing with miR-325-3p. In addition, the luciferase activity of the WT-TRPV4-3'UTR reporter was significantly decreased in miR-325-3p-transfected H9c2 cells under hypoxia conditions compared with the miR-NC group, whereas miR-325-3p displayed no significant effect on the luciferase activity of MUT-TRPV4-3'UTR compared with miR-NC (Fig. 5B). Additionally, the mRNA and protein expression levels of TRPV4 were significantly increased by hypoxia treatment in a time-dependent manner compared with normoxic H9c2 cells (Fig. 5C and D). In addition, the expression levels of miR-325-3p were significantly reduced in H9c2 cells transfected with anti-miR-325-3p compared with the anti-miR-NC group (Fig. 5E). Moreover, the mRNA and protein expression levels of TRPV4 were significantly reduced in the miR-325-3p group compared with the miR-NC group, but significantly upregulated in the anti-miR-325-3p group compared with the anti-miR-NC group (Fig. 5F and G). The results indicated

that TRPV4 was negatively regulated by miR-325-3p in hypoxia-treated H9c2 cells.

TRPV4 knockdown reduces hypoxia-induced injury in H9c2 cells via miR-325-3p. To investigate whether the effects of miR-325-3p on hypoxia-treated cardiomyocytes were mediated by TRPV4, si-TRPV4 and anti-miR-325-3p were co-transfected into hypoxia-treated H9c2 cells. The mRNA and protein expression levels of TRPV4 were significantly reduced in the si-TRPV4 group compared with the si-NC group, which was partially reversed by anti-miR-325-3p compared with anti-miR-NC (Fig. 6A and B). In addition, co-transfection with anti-miR-325-3p reduced si-TRPV4-mediated effects on cell viability in hypoxia-treated H9c2 cells (Fig. 6C). Additionally, the rate of apoptosis and LDH release were significantly downregulated in si-TRPV4-transfected H9c2 cells under hypoxic conditions compared with the si-NC group, but partially reversed in hypoxia-treated H9c2 cells co-transfected with si-TRPV4 and anti-miR-325-3p compared with the hypoxia + si-TRPV4 + anti-miR-NC group (Fig. 6D and F). Furthermore, the western blotting results demonstrated that anti-miR-325-3p reversed si-TRPV4-induced downregulation of Bax and cleaved caspase-3 protein expression levels, and attenuated si-TRPV4-mediated upregulation of Bcl-2 protein expression levels in hypoxia-treated H9c2 cells (Fig. 6E). The results indicated that downregulation of TRPV4 mitigated hypoxia injury in H9c2 cells by regulating miR-325-3p.

MEG3 upregulates TRPV4 expression in hypoxia-treated H9c2 cells by downregulating miR-325-3p. To assess the relationship among MEG3, miR-325-3p and TRPV4 in hypoxia-induced cardiomyocytes, MEG3 rescue experiments

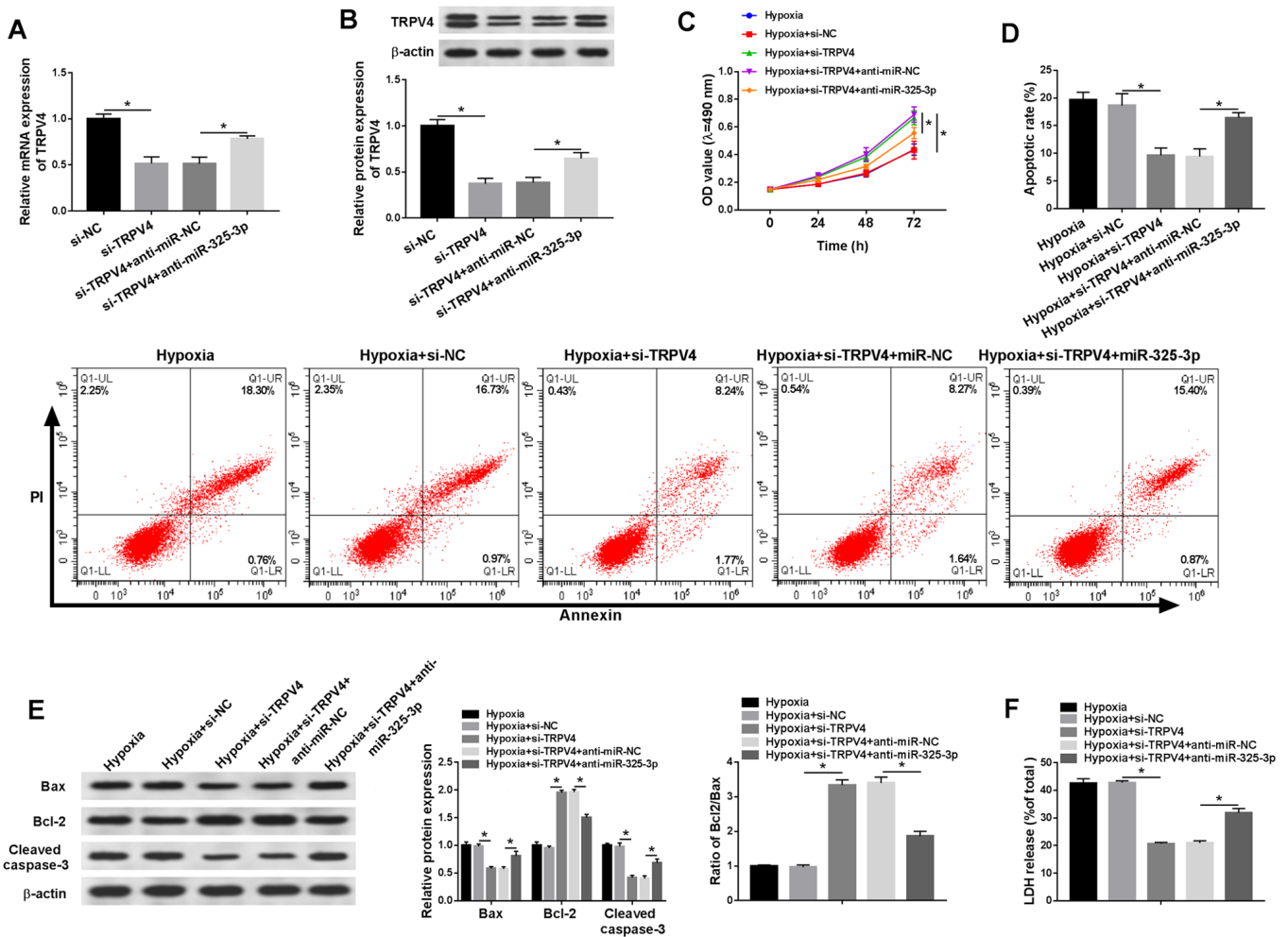


Figure 6. TRPV4 knockdown relieves hypoxia-induced injury in H9c2 cells via miR-325-3p. H9c2 cells were transfected with si-NC, si-TRPV4, si-TRPV4 + anti-miR-NC or si-TRPV4 + anti-miR-325-3p and then cultured in hypoxic conditions. TRPV4 (A) mRNA and (B) protein expression levels. (C) Cell viability was assessed by performing an MTT assay. (D) Cell apoptosis was measured via flow cytometry. (E) The protein expression levels of Bax, Bcl-2 and cleaved caspase-3 were measured via western blotting. (F) LDH release was measured by conducting the LDH determination assay. $n=3$. * $P<0.05$. TRPV4, transient receptor potential cation channel subfamily V member 4; miR, microRNA; si, small interfering RNA; NC, negative control; OD, optical density; LDH, lactate dehydrogenase.

were performed. Compared with the miR-NC group, the mRNA and protein expression levels of TRPV4 were significantly downregulated in miR-325-3p-transfected hypoxic H9c2 cells, but partly rescued in hypoxic H9c2 cells co-transfected with miR-325-3p and MEG3 compared with the hypoxia + miR-325-3p + vector group (Fig. 7A and B). The results demonstrated that MEG3 increased TRPV4 expression in hypoxia-treated H9c2 cells via miR-325-3p. In addition, the changes of MEG3, miR-325-3p and TRPV4 expression displayed no significant effect on the expression levels of HIF1 α in H9c2 cells (data not shown).

Discussion

Acute myocardial infarction, a primary threat to human health, causes cardiac cell death (17). A previous study revealed that lncRNAs serve important roles, including regulating vessel growth and function, controlling the contractile phenotype of smooth muscle cells, hypertrophy, mitochondrial function and apoptosis in cardiac diseases (18). The results of the present

study demonstrated that MEG3 regulated TRPV4 expression to reduce hypoxia-induced injury via miR-325-3p.

Accumulating evidence revealed that MEG3 is dysregulated in numerous complex diseases. For instance, a report on Alzheimer's disease demonstrated that MEG3 improved neuronal damage via the PI3K/AKT signaling pathway (19). Another study on non-alcoholic fatty liver disease reported that MEG3 was upregulated in high-content hydrogen water (HHW)-treated mice in contrast to the mice treated with deionized water, and MEG3 improved non-alcoholic fatty liver disease under HHW conditions via the miR-136/nuclear factor, erythroid 2 like 2 axis (20). The aforementioned results indicated that MEG3 serves different roles in different types of diseases. In the present study, MEG3 expression was significantly increased under hypoxic conditions compared with normoxic conditions. Compared with the si-NC group, MEG3 knockdown decreased the inhibitory effect of hypoxia on cell viability, and partially reversed the promoting effects of hypoxia on apoptosis and LDH release in H9c2 cells. The roles of MEG3 identified in the present study were consistent with

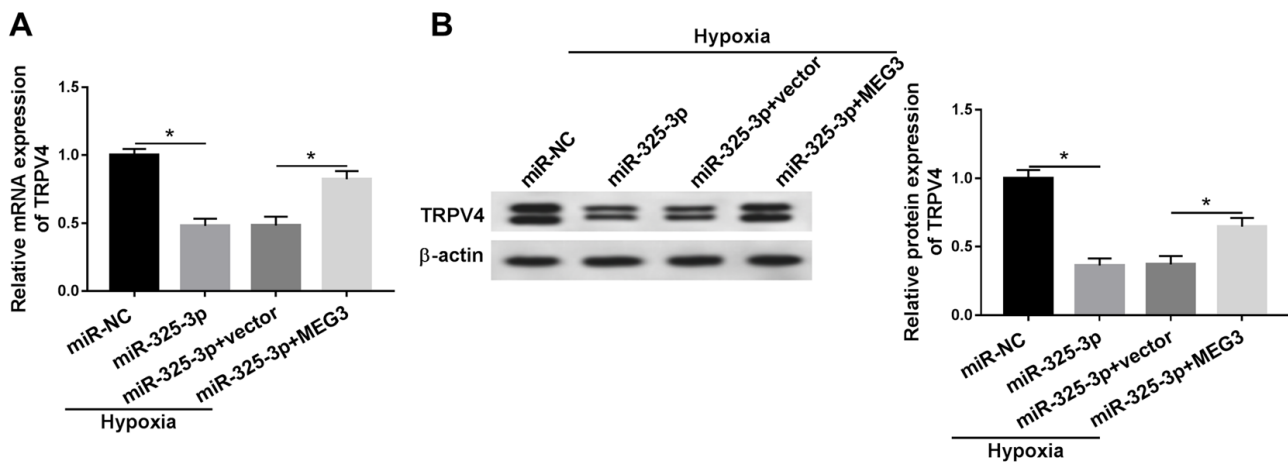


Figure 7. MEG3 upregulates TRPV4 expression in hypoxia-treated H9c2 cells by sponging miR-325-3p. TRPV4 (A) mRNA and (B) protein expression levels in hypoxia-treated H9c2 cells transfected with miR-NC, miR-325-3p, miR-325-3p + vector or miR-325-3p + MEG3. $n=3$. * $P<0.05$. MEG3, maternally expressed 3; TRPV4, transient receptor potential cation channel subfamily V member 4; miR, microRNA; NC, negative control.

previous studies (6,7), which indicated that MEG3 aggravated hypoxia-induced injury in AMI.

Previous studies demonstrated that miR-325-3p was implicated in cellular processes in different types of diseases. For example, Zhang *et al* (21) reported that miR-325-3p decreases aquaporin 5 expression to confine hepatitis B virus replication in hepatocellular carcinoma. Another study investigating hypoxic-ischemic brain damage indicated that miR-325-3p aggravates rat neonatal hypoxia-ischemia brain injury by modulating aralkylamine N-acetyltransferase (22). The results of the present demonstrated that miR-325-3p was sponged by MEG3 in hypoxia-treated H9c2 cells. Moreover, miR-325-3p expression levels were significantly decreased under hypoxic conditions compared with normoxic conditions. MEG3 regulated hypoxia-mediated effects on viability, apoptosis and LDH release in H9c2 cells via miR-325-3p. Similar results were reported in a previous study that also demonstrated that MEG3 facilitated hypoxia-stimulated injury by sponging miR-325-3p in myocardial infarction mouse model (11).

Accumulating evidence has indicated that the aberrant expression of TRPV4 was related to the development of heart diseases. For example, Wu *et al* (23) demonstrated that TRPV4 was significantly upregulated in the hypoxia/reoxygenation (H/R) model compared with a normal groups cultured in normoxic conditions, and accelerated cell injury in myocardial ischemia/reperfusion. Another study revealed that TRPV4 decreased cardiomyocyte stability in H/R conditions (24). In the present study, TRPV4 was negatively regulated by miR-325-3p, and the level of TRPV4 was significantly elevated in hypoxia-treated H9c2 cells compared with normoxic H9c2 cells. In addition, TRPV4 knockdown promoted cell viability, and reduced apoptosis and LDH release in hypoxia-treated H9c2 cells compared with si-NC. The aforementioned results of TRPV4 were consistent with a previous study that dysregulation of TRPV4 occurs in AMI (13). In addition, MEG3 modulated TRPV4 expression under hypoxic conditions by sponging miR-325-3p. The results suggested that MEG3 may regulate TRPV4 to aggravate hypoxia-induced injury in AMI by sponging miR-325-3p. Although the roles of MEG3, miR-325-3p and TRPV4 have been previously reported,

the present study suggested the regulatory network of the MEG3/miR-325-3p/TRPV4 axis in hypoxia-induced injury, which may aid with understanding the mechanisms underlying AMI development.

The present study had a number of limitations. First, only a rat cardiomyocyte cell line H9c2 was used. Although the H9c2 cell line is commonly used for the study of hypoxia-induced injury, two or more cardiomyocytes cell lines should be used to further verify the results of the present study. Second, the present study did not perform *in vivo* experiments. Therefore, future studies should employ other suitable cell lines and an established AMI mouse model.

In conclusion, the present study demonstrated that MEG3 and TRPV4 expression levels were significantly increased, and miR-325-3p expression levels were significantly decreased in hypoxic H9c2 cells compared with normoxic H9c2 cells. MEG3 knockdown relieved hypoxia-stimulated injury by downregulating TRPV4 expression via miR-325-3p. The results of the present study may aid with identifying the mechanism underlying AMI.

Acknowledgements

Not applicable.

Funding

No funding was received.

Availability of data and materials

The datasets used and/or analysed during the current study are available from the corresponding author on reasonable request.

Authors' contributions

YZ designed the study. YZ, XGL, DZ, XYL and JD performed the experiments. XGL and DZ analyzed the data. YZ and XGL wrote the manuscript. All authors read and approved the final manuscript.

Ethics approval and consent to participate

Not applicable.

Patient consent for publication

Not applicable.

Competing interests

The authors declare they have no competing interests.

References

- Anderson JL and Morrow DA: Acute myocardial infarction. *N Engl J Med* 376: 2053-2064, 2017.
- Li J, Li X, Wang Q, Hu S, Wang Y, Masoudi FA, Spertus JA, Krumholz HM, Jiang L: China PEACE Collaborative Group: ST-segment elevation myocardial infarction in China from 2001 to 2011 (The China PEACE-retrospective acute myocardial infarction study): A retrospective analysis of hospital data. *Lancet* 385: 441-451, 2015.
- Mathieu EL, Belhocine M, Dao L, Puthier D and Spicuglia S: Functions of lncRNA in development and diseases. *Med Sci (Paris)* 30: 790-796, 2014 (In French).
- Hu H, Wu J, Li D, Zhou J, Yu H and Ma L: Knockdown of lncRNA MALAT1 attenuates acute myocardial infarction through miR-320-Pten axis. *Biomed Pharmacother* 106: 738-746, 2018.
- Huang S, Tao W, Guo Z, Cao J and Huang X: Suppression of long noncoding RNA TTTY15 attenuates hypoxia-induced cardiomyocytes injury by targeting miR-455-5p. *Gene* 701: 1-8, 2019.
- Wu H, Zhao ZA, Liu J, Hao K, Yu Y, Han X, Li J, Wang Y, Lei W, Dong N, *et al*: Long noncoding RNA Meg3 regulates cardiomyocyte apoptosis in myocardial infarction. *Gene Ther* 25: 511-523, 2018.
- Gong L, Xu H, Chang H, Tong Y, Zhang T and Guo G: Knockdown of long non-coding RNA MEG3 protects H9c2 cells from hypoxia-induced injury by targeting microRNA-183. *J Cell Biochem* 119: 1429-1440, 2018.
- Huang Y, Shen XJ, Zou Q, Wang SP, Tang SM and Zhang GZ: Biological functions of microRNAs: A review. *J Physiol Biochem* 67: 129-139, 2011.
- Chen Y, Zhao Y, Chen W, Xie L, Zhao ZA, Yang J, Chen Y, Lei W and Shen Z: MicroRNA-133 overexpression promotes the therapeutic efficacy of mesenchymal stem cells on acute myocardial infarction. *Stem Cell Res Ther* 8: 268, 2017.
- Zhang M, Cheng YJ, Sara JD, Liu LJ, Liu LP, Zhao X and Gao H: Circulating microRNA-145 is associated with acute myocardial infarction and heart failure. *Chin Med J (Engl)* 130: 51-56, 2017.
- Zhang DY, Wang BJ, Ma M, Yu K, Zhang Q and Zhang XW: MicroRNA-325-3p protects the heart after myocardial infarction by inhibiting RIPK3 and programmed necrosis in mice. *BMC Mol Biol* 20: 17, 2019.
- Grace MS, Bonvini SJ, Belvisi MG and McIntyre P: Modulation of the TRPV4 ion channel as a therapeutic target for disease. *Pharmacol Ther* 177: 9-22, 2017.
- Rath G, Saliez J, Behets G, Romero-Perez M, Leon-Gomez E, Bouzin C, Vriens J, Nilius B, Feron O and Dessy C: Vascular hypoxic preconditioning relies on TRPV4-dependent calcium influx and proper intercellular gap junctions communication. *Arterioscler Thromb Vasc Biol* 32: 2241-2249, 2012.
- Livak KJ and Schmittgen TD: Analysis of relative gene expression data using real-time quantitative PCR and the 2(-Delta Delta C(T)) method. *Methods* 25: 402-408, 2001.
- Kietzmann T, Samoylenko A, Roth U and Jungermann K: Hypoxia-inducible factor-1 and hypoxia response elements mediate the induction of plasminogen activator inhibitor-1 gene expression by insulin in primary rat hepatocytes. *Blood* 101: 907-914, 2003.
- Yu B and Wang W: Cardioprotective effects of morroniside in rats following acute myocardial infarction. *Inflammation* 41: 432-436, 2018.
- Qiu H, Liu JY, Wei D, Li N, Yamoah EN, Hammock BD and Chiamvimonvat N: Cardiac-generated prostanoids mediate cardiac myocyte apoptosis after myocardial ischaemia. *Cardiovasc Res* 95: 336-345, 2012.
- Uchida S and Dimmeler S: Long noncoding RNAs in cardiovascular diseases. *Circ Res* 116: 737-750, 2015.
- Yi J, Chen B, Yao X, Lei Y, Ou F and Huang F: Upregulation of the lncRNA MEG3 improves cognitive impairment, alleviates neuronal damage, and inhibits activation of astrocytes in hippocampus tissues in Alzheimer's disease through inactivating the PI3K/Akt signaling pathway. *J Cell Biochem* 120: 18053-18065, 2019.
- Wang X and Wang J: High-content hydrogen water-induced downregulation of miR-136 alleviates non-alcoholic fatty liver disease by regulating Nrf2 via targeting MEG3. *Biol Chem* 399: 397-406, 2018.
- Zhang Z, Han Y, Sun G, Liu X, Jia X and Yu X: MicroRNA-325-3p inhibits cell proliferation and induces apoptosis in hepatitis B virus-related hepatocellular carcinoma by down-regulation of aquaporin 5. *Cell Mol Biol Lett* 24: 13, 2019.
- Yang Y, Sun B, Huang J, Xu L, Pan J, Fang C, Li M, Li G, Tao Y, Yang X, *et al*: Up-regulation of miR-325-3p suppresses pineal aralkylamine N-acetyltransferase (Aanat) after neonatal hypoxia-ischemia brain injury in rats. *Brain Res* 1668: 28-35, 2017.
- Wu QF, Qian C, Zhao N, Dong Q, Li J, Wang BB, Chen L, Yu L, Han B, Du YM and Liao YH: Activation of transient receptor potential vanilloid 4 involves in hypoxia/reoxygenation injury in cardiomyocytes. *Cell Death Dis* 8: e2828, 2017.
- Gorbunov AS, Maslov LN, Jaggi AS, Singh N, De Petrocellis L, Boshchenko AA, Roohbakhsh A, Bezuglov VV and Oeltgen PR: Physiological and pathological role of TRPV1, TRPV2 and TRPV4 channels in heart. *Curr Cardiol Rev* 15: 244-251, 2019.



This work is licensed under a Creative Commons Attribution-NonCommercial-NoDerivatives 4.0 International (CC BY-NC-ND 4.0) License.